



# Silica-modified magnetic nanoparticles functionalized with cetylpyridinium bromide for the preconcentration of metals after complexation with 8-hydroxyquinoline

Andreas E. Karatapanis, Yiannis Fiamegos, Constantine D. Stalikas\*

University of Ioannina, Department of Chemistry, Ioannina 45110 Greece

## ARTICLE INFO

### Article history:

Received 5 November 2010

Received in revised form 28 January 2011

Accepted 14 February 2011

Available online 19 February 2011

### Keywords:

Magnetic nanoparticles

8-Hydroxyquinoline

Cetylpyridinium bromide

Microextraction of metals

Atomic absorption spectrometry

## ABSTRACT

Magnetically driven separation technology has received considerable attention in recent decade for its great potential application. In this study, we investigate the application of silica-modified magnetite nanoparticles (NPs) coated with a cationic surfactant as adsorbent for microextraction and determination of trace amounts of Cu(II), Ni(II), Co(II), Cd(II), Pb(II) and Mn(II) from environmental water samples. The synthesized silica-coated NPs in combination with cetylpyridinium bromide have the ability to adsorb the metal ions after complexation with 8-hydroxyquinoline. The NPs bearing the target metals are easily separated from the aqueous solution by applying an external magnetic field and the complexed metals were desorbed using acidic methanol. The desorbed analytes are introduced into the graphite furnace of an atomic absorption spectrometer. The effect of pH, complexing agent, amount of cetylpyridinium bromide, microextraction time, desorption conditions, ionic strength on extraction efficiency of the metal ions are investigated and optimized. Under the optimized conditions, the detection limits for Cu(II), Ni(II), Co(II), Cd(II), Pb(II) and Mn(II) are 4.7, 9.1, 9.5, 2.3, 7.4 and 15.3 ng L<sup>-1</sup>, respectively and the relative standard deviations ( $n=6$ ) are less than 3.6%. The accuracy of the method was evaluated by recovery measurements on the spiked samples and good recoveries (93–113%) with low RSDs were achieved.

© 2011 Elsevier B.V. All rights reserved.

## 1. Introduction

Iron-oxide magnetic nanoparticles (NPs) have been showing a worldwide growing research interest as they possess unique size-dependent characteristics that strongly differ from the properties of the corresponding bulk material and enable them to be used for numerous applications [1]. Magnetite (Fe<sub>3</sub>O<sub>4</sub>) and maghemite (γ-Fe<sub>2</sub>O<sub>3</sub>) are heralded as suitable iron-oxide NPs due to their biocompatibility, low toxicity and strong magnetization response [2]. Magnetite can be converted to maghemite by chemical oxidation, which results in a color change from black to red-brown and a slightly reduced saturation magnetization. Iron-oxide magnetic NPs are superparamagnetic, which means that being adhered to the target compounds they can be removed along with them from a matrix quickly, using a magnetic field. These characteristics make them highly useful in novel separation processes. Maghemite, for instance, has been reported for the successful removal of heavy metals such as Cr(VI) [3] and As(V) [4] from wastewater.

Inorganic magnetic NPs (such as Fe<sub>3</sub>O<sub>4</sub> and γ-Fe<sub>2</sub>O<sub>3</sub>) are prone to the formation of aggregates thus altering their magnetic properties in complex matrixes. Although iron oxides are relatively inert, in chemical terms, functionalized magnetic NPs have been described, which retain the desired magnetic properties and are stable in aqueous colloidal suspensions.

Iron-oxide magnetic NPs modified with oleic acid and undecanoic acid have been used for capturing As(III)–As(V) [5] and Cd [6] while dispersible thiol functionalized magnetite NPs have been described for the removal of heavy metals from aqueous systems [7]. Likewise, functionalized magnetic NPs have been reported for the isolation, identification and quantification of small molecules with matrix-assisted laser desorption/ionization time-of-flight mass spectrometry [8].

Surface modification by silanization is also a very common method for particle functionalization. Silica has been considered as one of the most ideal shell materials due to its reliable chemical stability and versatility in surface modification via Si–OH groups [9–11]. Along these lines, modified silica-coated magnetite NPs have been used for the analysis of estrogens [12] and the selective extraction of trace amounts of Cd, Cu, Hg and Pb [13] and Cu, Fe, and Pb [14], exploiting the complexation of metals with thiol and their affinity to amino groups, respectively.

\* Corresponding author. Tel.: +30 2651008414; fax: +30 2651008796.  
E-mail address: [cstaliika@cc.uoi.gr](mailto:cstaliika@cc.uoi.gr) (C.D. Stalikas).

Apart from silica modification, other suitable coatings on the surface of the particles have frequently been developed to overcome limitations and to improve their colloidal and chemical stability [15]. In this vein, surfactants can be employed in order to be chemically anchored or physically adsorbed on NPs, thus forming a single or a double layer. This layer creates repulsive forces to balance the magnetic and the van der Waals attractive forces, which act on NPs [16]. The outer surface of the hemimicelles and admicelles formed on the surface of metal oxides is hydrophobic and ionic, respectively, providing a dual mechanism for the retention of organics and the preconcentration of organic compounds, in solid-phase extraction mode [17–20]. However, in case of microparticles, this preconcentration mode may have a relatively low extraction capability as well as being time-consuming when a large sample volume is loaded. These drawbacks can be overcome with magnetic NPs, which have high surface area and strong magnetism [21]. The functionalization of bare and silica-coated magnetic NPs – usually magnetite – with a single or double layer of surfactants has resulted in stable colloidal dispersions for several microextraction purposes [22–26].

Surfactants have widely been used for the analysis of metals using cloud-point extraction [27,28]. In this paper, capitalizing on (a) the negative charge of silica-coated iron-oxide magnetic NPs in a broad pH range, (b) the property of cationic surfactants to adsorb onto these surfaces and to eliminate their agglomeration and (c) the capability of the adsorbed surfactants to solubilize hydrophobic molecules – the so-called adsolubilization process – we put forward the concept of the preconcentration of complexed metal ions on nanometer-sized silica-modified magnetite functionalized with the cationic cetylpyridinium bromide (CPBr). More specifically, certain metal ions form stable complexes with 8-hydroxyquinoline (8-HQ) [29], which can be adsorbed on surfactant-coated magnetic NPs, in a batch microextraction procedure. The magnetic NPs are then collected using an external magnetic field and the extracted metal ions are eluted and determined by electrothermal atomic absorption spectrometry (ETAAS). To the best of our knowledge, it is the first work to use CPBr-coated magnetic NPs for the microextraction–preconcentration of complexed metals from aqueous samples based on mixed hemimicelles–admicelles.

## 2. Experimental

### 2.1. Materials

Stock standard solutions of Pb(II), Cd(II), Mn(II), Cu(II), Ni(II), Co(II) ( $1000 \pm 2 \text{ mg L}^{-1}$  each) were purchased from Merck (Darmstadt, Germany). Suprapur grade  $\text{HNO}_3$  used in the experiments was obtained from Merck (Darmstadt, Germany). Diluted solutions of each metal were prepared in 2%  $\text{HNO}_3$ . Tetraethyl orthosilicate (TEOS) 99% was obtained from Aldrich (Sigma–Aldrich Ltd., Greece). The 8-HQ (99%, Sigma–Aldrich Ltd., Greece) solution was prepared daily by dissolving the solid chemical in acetic acid (TraceSelect, Fluka Chemie, Buchs, Switzerland), under sonication. Cetylpyridinium bromide (CPBr) 97% (Fluka), at a concentration  $2 \times 10^{-2} \text{ M}$  was prepared in DDW, under slight heating. Palladium nitrate in nitric acid was obtained from Merck (Darmstadt, Germany) and used as matrix modifier solution for electrothermal atomization. Other reagents, including  $\text{FeCl}_3 \cdot 6\text{H}_2\text{O}$ ,  $\text{FeCl}_2 \cdot 4\text{H}_2\text{O}$  (99.99% trace metal basis),  $\text{NaNO}_3$ ,  $\text{NaOH}$  and  $\text{NH}_3$  were of analytical grade and obtained from Sigma–Aldrich (Sigma–Aldrich Ltd., Greece).

### 2.2. Synthesis of magnetite and silica-modified magnetite NPs

Magnetite NPs and the silica modified counterpart were prepared according to a slightly modified reported coprecipitation

method [30]. An aliquot of 25%  $\text{NH}_4\text{OH}$  was added into a vigorously stirred deoxygenated aqueous solution of  $\text{FeCl}_2 \cdot 4\text{H}_2\text{O}$  ( $1.5 \times 10^{-3} \text{ mol L}^{-1}$ ) and  $\text{FeCl}_3 \cdot 6\text{H}_2\text{O}$  ( $3.0 \times 10^{-3} \text{ mol L}^{-1}$ ) until obtaining a pH of 10, at room temperature. The black precipitate of magnetite NPs formed under continuous flow of nitrogen was immediately separated from the supernatant by a magnet and redispersed in aqueous solution, at least three times, until obtaining pH 7, washed twice with ethanol and evaporated to dryness to get the magnetite powder. The obtained magnetic powder was  $\sim 240 \text{ mg}$ . After that, the surface of the particles was alternatively coated with TEOS. The procedure consisted of placing 50 mL of ethanol and 4 mL of DDW into a beaker containing 100 mg of magnetite NPs. Then, the pH of the suspension was adjusted to 9.0 with  $\text{NH}_3$  and 200  $\mu\text{L}$  of TEOS were added followed by overnight stirring, under nitrogen. After magnetic separation, the silanized magnetic particles were thoroughly washed with DDW and dried, yielding a fine powder.

### 2.3. Characterization

#### 2.3.1. Surface area

The surface areas of the bare and modified iron-oxide NPs were determined by nitrogen adsorption–desorption porosimetry according to the BET method. The samples were tested for their surface area, porosity and mean diameter by  $\text{N}_2$  adsorption–desorption porosimetry, at 77 K in an Autosorb-1 Quantachrome porosimeter. Before measurement, each sample was degassed at  $80^\circ\text{C}$ , for 5 h. The partial pressure of nitrogen in the mixture was varied from 40 to 250 Torr.

#### 2.3.2. FT-IR spectroscopy

The FT-IR spectra of the bare and silanized magnetite NPs were recorded on a Perkin-Elmer Spectrum GX FT-IR spectrophotometer with samples as KBr pellets. The KBr wafers were prepared by mixing KBr crystals with sample, dried previously at 373 K for 24 h and ground to fine powder.

#### 2.3.3. Determination of point of zero charge (pHPZC) of NPs by the salt addition method

The point of zero charge (pHPZC) of the bare and silanized magnetite NPs was determined in degassed 0.01 M  $\text{NaNO}_3$  solutions, at  $20^\circ\text{C}$ . Thirty mL of 0.01 M  $\text{NaNO}_3$  solutions were taken and mixed with 30 mg of NPs, in different beakers. The pH values of the solutions were adjusted to 2, 3, 4, 5, 6, 7, 8, 9 using solutions of  $\text{HNO}_3$  and  $\text{NaOH}$ . The initial pH of the solution was recorded with a pH meter (Radiometer PHM83 Autocal pH meter, Copenhagen) and each flask was covered with parafilm and shaken for 24 h. The final pH values of the solutions were recorded and the difference between initial and final pH – the so-called  $\Delta\text{pH}$  – was plotted against the initial pH values. The pHPZC values were calculated from  $\Delta\text{pH}$  versus pH plots, at the pH where  $\Delta\text{pH} = 0$ .

#### 2.3.4. Surface charge of the synthesized NPs

The surface charges of both iron oxide materials were based on potentiometric titrations, conducted at  $20^\circ\text{C}$ . Thirty mL background electrolyte ( $\text{NaNO}_3$ ) solutions of concentration 0.01 M each containing 30 mg of NPs were equilibrated for 30 min, under continuous stirring. Nitrogen gas was constantly passed through the suspension to bubble out the  $\text{CO}_2$ . Following equilibration, 2 mL of 0.1 N  $\text{HNO}_3$  were added and the suspension was further stirred for 20 min. The new pH value of the suspension was recorded with the pH meter. The suspension was then titrated by the addition of 0.05 M  $\text{NaOH}$  delivered by a micro-burette (ABU80 Autoburette, Radiometer, Copenhagen) of very fine tip. After each addition of base, the suspension was equilibrated for 1 min with stirring, at the end of which the changes were less than  $0.01 \text{ pH units min}^{-1}$ .

A blank titration was also performed with similar solutions in the absence of the oxide.

The surface charge of the NPs, defined as the portions of the surface charge due to  $\text{OH}^-$  and  $\text{H}^+$ , were calculated from the potentiometric titration curves according to the relationship [31]:

$$\sigma_o = \frac{F(n_a - n_b + n_{\text{OH}} - n_{\text{H}})}{S}$$

where  $\sigma_o$  is the surface charge density ( $\text{C m}^{-2}$ ),  $F$  is the faraday constant ( $\text{C mol}^{-1}$ ),  $n_a$  and  $n_b$  are the moles of the acid and base added to the suspension,  $n_{\text{OH}}$  and  $n_{\text{H}}$  are the numbers of moles of  $\text{OH}^-$  and  $\text{H}^+$  in the suspension at a measured pH and  $S$  is the total surface area of the oxide.

#### 2.4. Adsorption of CPBr on NPs

The adsorption isotherms of CPBr on NPs were determined by batch experiments, at constant electrolyte concentration ( $0.01 \text{ M NaNO}_3$ ). Suspensions containing  $10 \text{ mg}$  of NPs were stirred for  $3 \text{ min}$  with a series of solutions containing increasing amounts of CPBr, at room temperature and then they were equilibrated for  $10 \text{ min}$ . The pH was adjusted to  $8.5 \pm 0.1$  by adding small portions of  $0.1 \text{ M NaOH}$ . The NPs were isolated using a magnet at the bottom of the container and the concentration of CPBr in the limpid supernatant was determined spectrophotometrically on a Shimadzu UV-2100 spectrophotometer, at  $260 \text{ nm}$ . Linearity between the absorbance and CPBr concentrations was obtained in the range  $0.5\text{--}60 \text{ mg L}^{-1}$ , with a correlation coefficient of  $0.9996$ .

The critical micelle concentration (cmc) of CPBr was taken as  $9.0 \times 10^{-4} \text{ mol L}^{-1}$  [32] corresponding to  $345 \text{ mg L}^{-1}$ .

#### 2.5. NPs-based microextraction of complexed metals

Two solutions were prepared for the microextraction of metal ions:

**Solution A.** An aliquot of  $1 \text{ mL}$  of  $8\text{-HQ}$   $1.3\%$  was added to a beaker containing  $100 \text{ mL}$  of an aqueous solution with metals. The pH was adjusted to  $8.5$  with  $0.1 \text{ M NaOH}$  and the solution was stirred for  $15 \text{ min}$ , at room temperature.

**Solution B.** A suspension of silica-modified magnetite NPs ( $10 \text{ mg mL}^{-1}$ ), which contained  $30 \text{ mg mL}^{-1}$  CPBr was prepared at pH  $8.5$ . After vigorous stirring the suspension was equilibrated for  $10 \text{ min}$ .

An aliquot of  $1 \text{ mL}$  of solution B was added to the solution A and the mixture was stirred for  $3 \text{ min}$ . The beaker was placed on a magnet for around  $2 \text{ min}$ , to let NPs settle down. The supernatant was removed by decantation and the isolated NPs were eluted with  $250 \mu\text{L}$  of methanolic solution of  $1 \text{ N HNO}_3$  to desorb the complexed metals. A portion of the acidic methanolic eluent was then injected directly into ETAAS for analysis. Palladium solution was used as modifier for Cd and Pb.

#### 2.6. Measurement of metals

The ETAAS measurements were carried out on a GBC AAS 932 Plus, equipped with a GF3000 Graphite Furnace System and a PAL 3000 Auto Sampler GBC Scientific Pty. Ltd. (Victoria, Australia). The control of the AAS system and the evaluation of the data received were carried out by means of GBC Avanta 2.01 Software, (copyright 1996, GBC Scientific Equipment Pty, Ltd.). A multielement hollow-cathode lamp for cadmium, lead, nickel, manganese and copper and a single element hollow-cathode lamp for cobalt were from Proton Pty. Ltd. (Victoria, Australia).

**Table 1**

Morphological characteristics of magnetite and silanized magnetite NPs.

NPs	Specific surface area ( $\text{m}^2 \text{ g}^{-1}$ )	Total pore volume ( $\text{cm}^3 \text{ g}^{-1}$ )
Magnetite	167	0.54
Silanized magnetite	168	0.51

### 3. Results and discussion

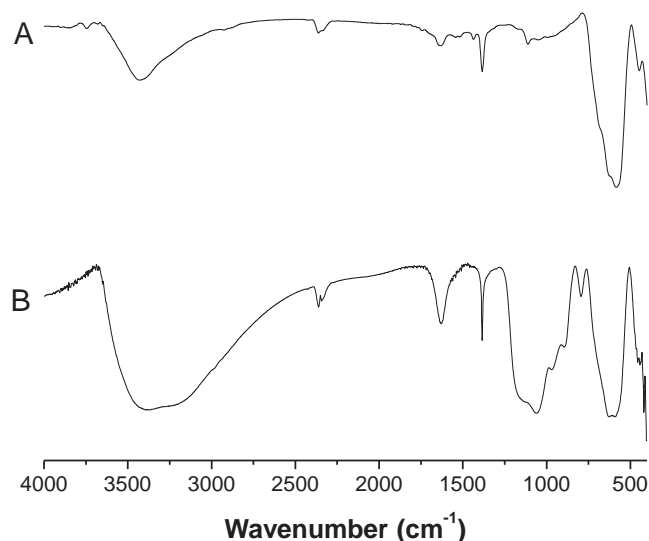
#### 3.1. Characterization of the synthesized magnetic NPs

Table 1 lists the porosity and surface area of the synthesized NPs, which were determined by nitrogen sorption measurements (relevant isotherms are provided in Fig. S1 of Supplementary Material). The surface areas of bare and silanized magnetite were found to be  $167$  and  $168 \text{ m}^2 \text{ g}^{-1}$ , respectively. It can also be seen that the specific surface areas and total pore volume were not obviously different between iron oxide and the silica-modified NPs. Therefore, the process of silanization does not influence the above characteristics of the sorbents and any differences in the subsequent study between them cannot be attributed to the morphological differences.

##### 3.1.1. FT-IR spectra of NPs

The production of iron oxide NPs can be seen from the occurrence of a strong absorption band in the FT-IR spectrum, which encompasses the characteristic wavenumbers of  $632$  and  $585 \text{ cm}^{-1}$  (Fig. 1A). This pattern corresponds to the Fe–O bonds, which is reported to belong to bulk magnetite [33]. In addition, the final product obtained from the coprecipitation was dense, black and magnetic implying the presence of magnetite as the main phase.

The deposition of silica network on the magnetite surface by Fe–O–Si bonds through silanization was also confirmed by obtaining relevant FT-IR spectrum. The corresponding absorption band cannot be seen in the FT-IR spectrum because it appears at around  $584 \text{ cm}^{-1}$  and inevitably overlaps with the Fe–O vibration of magnetite [34]. However, the strongly absorbing region of  $1110\text{--}1000 \text{ cm}^{-1}$  in the spectrogram of Fig. 1B results from the vibration of Si–O–H and Si–O–Si groups. To further confirm that the magnetite NPs are indeed protected by silica coating, silanized particles were immersed for  $24 \text{ h}$ , in two solutions: (a)  $1 \text{ M NaOH}$  and (b)  $1 \text{ M HCl}$ , in order to assess the dissolution of silicates and leaching of iron, respectively. Using the heteropoly blue method



**Fig. 1.** FT-IR spectra of (A) magnetite NPs and (B) silica-modified magnetite NPs.

[34] a deep blue color was formed from the alkaline solution, which revealed the presence of silicate arising from the dissolution of the silanized particles. At the same time, using flame AAS, iron was hardly detected in the acidic solution, which implies that the leaching of iron out of the silica layer is insignificant. Additionally, it was noticed that the leaching of iron in the acidic solution was heightened as the concentration of TEOS was getting lower, at the stage of silanization. Therefore, under the stated conditions of silanization, the resulting magnetite was properly protected by silica coating.

### 3.1.2. Point of zero charge of NPs

It is well known that the surface charge of oxides due to hydroxyl groups is largely dependent on the pH of the solution, the pHPZC caused by the amphoteric behavior of hydroxylated surface groups and the interaction between surface sites and the electrolyte species [35]. The addition, in either form, of the synthesized magnetite to the  $\text{NaNO}_3$  solution, causes changes in the pH, which were measured at a constant ionic strength. The  $\Delta\text{pH}$ , when plotted against the initial pHs, yield the pHPZC at a pH where  $\Delta\text{pH} = 0$  (plots are shown in Fig. S2 of Supplementary Material). The pHPZC of synthesized magnetite NPs was located close to pH 6 and that of silica-coated magnetite NPs was at pH 3, both being consistent with reported values [24,26]. The surface charge is neutral at the pHPZC. When the pH value exceeds the pHPZC the surface is negatively charged and adsorption of cations occurs because of the attractive electrostatic effect. Surface coverage of the magnetite with silica, reasonably, leads to a decrease in the pHPZC of the surface approaching the respective value of pure silica. Differences reported in the synthesis procedures, aqueous medium conditions and measuring methods are likely to be the cause of the different pHPZC. Actually, lower concentrations of TEOS in the silanization procedure described above, gave rise to higher pHPZC for the produced silica-coated magnetite. The incomplete surface coating results in a non-homogeneous surface chemical composition, which would affect the pHPZC of the silanized magnetite.

### 3.1.3. Surface charge of synthesized NPs

As mentioned above, magnetite and its silanized counterpart, as amphoteric solids, can develop charges in the protonation and deprotonation reactions of  $\equiv\text{FeOH}$  and  $\equiv\text{SiOH}$  surface sites. In the absence of specific adsorbing CPBr cations, the surfaces are negatively charged at any  $\text{pH} > \text{pHPZC}$ . The net charge of the synthesized NPs was determined from acid–base titrations (plots are shown in Fig. S3 of Supplementary Material). In the pH range of 6–9, the density of negative charges on the surfaces rises rapidly. Moreover, the charge of the silanized magnetite NPs is at least twice as that in bare magnetite, at constant electrolyte concentration (0.01 M  $\text{NaNO}_3$ ).

## 3.2. Mixed hemimicelle-based microextraction of metals

### 3.2.1. CPBr adsorption on NPs

CPBr was the cationic surfactant of choice for the adsolubilization of complexed metals because of its high load on silica particles [19] and its facile determination in solutions by UV spectroscopy.

The adsorption isotherms of CPBr on the synthesized NPs were important to understand the extraction mechanism and to optimize the conditions for metal preconcentration. Isotherms for both NPs were determined, for reasons of comparison, at pH 8.5, where high surface density occurs but not at higher pH values in order to avoid hydrolysis of silica shell. The amounts of the adsorbed surfactant plotted as a function of the equilibrium concentrations of CPBr are shown in Fig. 2. CPBr has almost similar adsorption behavior for both NPs. However, the maximum adsorbed amount of CPBr on magnetite (Fig. 2A) is approximately half that on the silanized counterpart (Fig. 2B). The CPBr can be adsorbed on magnetite NPs, since surface interactions may exist between the positively charged

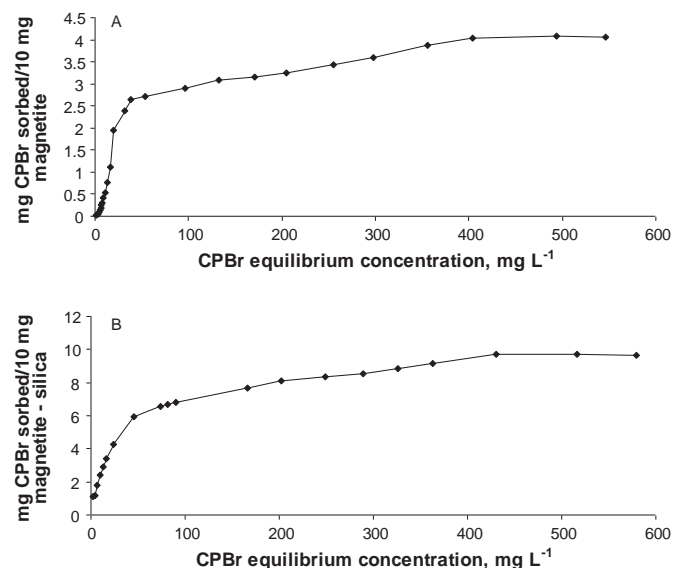


Fig. 2. Adsorption isotherms for CPBr on: (A) magnetite and (B) silica-modified magnetite NPs, at pH 8.5.

head group of CPBr and the  $\equiv\text{FeOH}$  and  $\equiv\text{SiOH}$  sites, on the surface of NPs. Therefore, the difference in the sorbed amounts is most likely attributed to the more dense surface charge of the latter and to the specific interactions of CPBr and the surface of the oxide, at a constant salt concentration [36].

The greatest proportions of the CPBr adsorbed on the surface of magnetite NPs and silanized counterpart are up to 2.5 mg/10 mg and 6 mg/10 mg, respectively. This region is considered as hemimicelles, in which CPBr molecules are adsorbed on the oppositely charged NPs surface to form single layer through coulombic attraction. The adsorption amount of CPBr on the NPs increased gradually with an increase in the amount of the cationic surfactant added to the solution, as a result of the gradual formation of bilayers (admicelles) by hydrophobic interaction between the alkyl chains. This region, where hemimicelles and admicelles coexist in equilibrium with aqueous surfactant monomers is termed as mixed hemimicelles/admicelles. Further increase in CPBr concentration did not increase the adsorbed amount indicating that aqueous micelles dominate. In this region, the analytes may be absorbed into micelles in bulk solution, which makes the isotherm span unsuitable for microextraction applications.

Finally, noteworthy is the formation of micelles in the solution for both nanosized materials before the adsorption of the surfactants has leveled off. This has been reported as a commonplace in alkylpyridinium halides adsorbed on microsize silica particles [19].

### 3.2.2. Study of the pH of working solution

The pH is critical for the system under investigation because it influences directly two distinctive processes: (a) the formation of metal-complexes in the solution and (b) the adsorption of the cationic surfactant on the NPs due to variation in the surface charge. The effect of pH on the signal intensity of metal ions was studied with pH varying from 3.0 to 9.0. Neither bare magnetite NPs nor silica-modified counterpart exhibited any obvious recovery of metal ions at pH values up to 4.0. With the increase of pH, the adsorption efficiency of the analytes improved dramatically and reached a maximum at a pH above 8.0. This is due to the combined effects of the formation of metal complexes at high pH values and the development of the negative charges, which were favorable for the adsorption of the cationic CPBr.



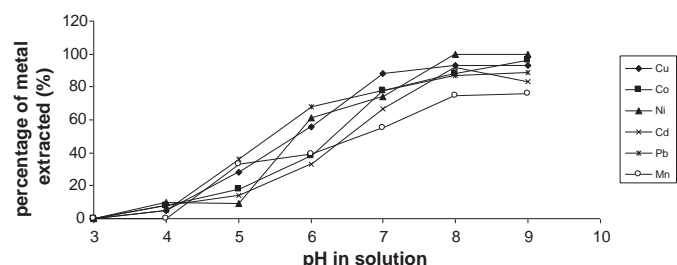


Fig. 3. Effect of pH on the pre-concentration of metal ions into mixed hemimicelles developed on silanized magnetite NPs.

Although the interactions between the CPBr and the surfaces have been reported to be favorable within a wide range of pH [19,23], it has been proven that the higher the pH value the larger the charge density of the mineral oxide and hence the more positive the effect of adsolubilization on the complexed metals. At high alkaline pH values, metal ions can precipitate as hydroxides and the pre-concentration on the NPs is not favoured since the preferred complexes are not formed. In addition, at alkaline conditions, the potential formation of cationic ammonium complexes may deter the adsorption of the heavy metal ions on the positively charged surface of the adsorbent. Taking into account that high charge density for magnetite occurs at elevated pH values, that kind of the synthesized adsorbent was not studied further. As regards silica-modified NPs, to avoid hydrolysis of the silica substrate with concomitant loss of adsorption properties, a pH of 8.5 was finally selected for subsequent experiments. The experimental results for silica-modified magnetite NPs are portrayed in Fig. 3.

### 3.2.3. Effect of the amount of CPBr on microextraction of complexed metals

Numerous microextraction processes take advantage of the interaction of analytes with the hemimicelles/admicelles phase on surfaces, which is driven by both hydrophobic and electrostatic interactions. In the study herein, the complexed metal species, being in neutral form, can only be retained by way of the hydrophobic interactions. From Fig. 4, we can note that in the absence of surfactant, the proportion of the complexed metals, which are adsorbed onto the surface of silanized magnetite NPs was almost undetectable. That is, the ion exchange of the charged metallic species with the negative surface of NPs is practically absent, given the complexation of metals is complete. The adsorbed amount of complexed metals increased markedly with increasing the amount of CPBr added and the maximum adsorption was obtained when CPBr was between 1.5 and 4 mg/10 mg of NPs. This amount is below the corresponding cmc of CPBr and represents the domain, where hydrophobic mixed hemimicelles (hemimicelles and admicelles) are formed on the surface of NPs. Further increase in CPBr above the cmc caused a gradual decrease in the adsorption of metal ions.

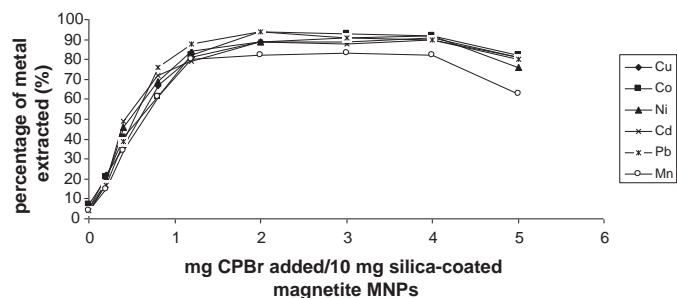


Fig. 4. Effect of the amount of CPBr added on the extraction of complexed metal ions at pH 8.5.

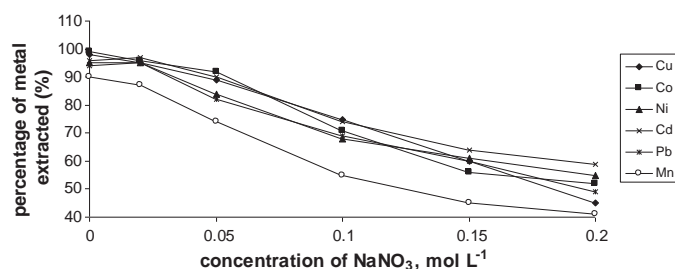


Fig. 5. Effect of ionic strength on the adsorption percentages of metal ions on silica-modified magnetite NPs.

This should be attributed to the formation of CPBr micelles in the bulk aqueous solution, which causes the complexed metals to redistribute again into the solution. Taking into account these findings, 3 mg/10 mg of NPs was selected as the final addition amount of CPBr for the subsequent studies.

### 3.2.4. Study of the concentration of 8-HQ

8-Hydroxyquinoline is a well known complexing agent that forms complexes with many metal ions. Advantages of 8-HQ as chelating reagent can be summarized as follows: (a) It is known to react with over 60 metal ions forming complexes [formation constants in the range  $10^4$  (Ba(II)) to  $10^{38}$  (Fe(III))] [37] (b) metal ion complexes with 8-HQ are sparingly soluble in water.

The variation of the analytical signals of metal ions was studied as a function of the concentration of 8-HQ in the range of 0–1.5 mmol L<sup>-1</sup>, for a total metal concentration of 10 µg L<sup>-1</sup>, at pH 8.5. The results (data not shown) demonstrated that the analytical signals of metal ions were accentuated by the 8-HQ at a concentration up to 0.85 mmol L<sup>-1</sup>. In the absence of the complexing agent, metals were hardly adsorbed on silicate magnetite, no matter what their chemical forms are, at the working pH. To compensate for potential complexation of 8-HQ with other foreign ions in the sample, the complexation at low parts per billion concentrations of metal ions of interest was effectively realized using 1.0 mmol L<sup>-1</sup> of 8-HQ.

### 3.2.5. Microextraction time and amount of silanized magnetite NPs

The total microextraction time relates to the time required for the complexation reaction and the transfer of hydrophobic complexes to silanized magnetite through adsolubilization. The effect of microextraction time on the overall microextraction efficiency of the heavy metal ions was studied with periods of time to vary in the range of 2–20 min. It was observed that after 15 min of reaction time at room temperature and 3 min of standing time, in the presence of CPBr and NPs, the recoveries of the heavy metal ions exhibited no obvious variation. Moreover, 10 mg of silanized magnetite NPs being covered with mixed hemimicelles/admicelles of CPBr were enough to preconcentrate the metal ions, at the studied concentrations, using 100 mL of sample. The demand for low amounts of nanosized adsorbent is reasonably attributed to the pronouncedly higher surface area of nanosized materials as compared to the classical microsized ones. For higher amounts of silanized magnetic NPs, the extraction efficiency was almost constant even at increased concentrations of CPBr.

### 3.2.6. Desorption conditions

Organic solvents are known to cause disruption of surfactant aggregates [28]. On the other hand, when the pH drops well below the pHPZC, the surface of silica-coated magnetite is rendered positive and amenable to disruption of surfactant molecules already aggregated on the surface. Therefore, it is not surprising that the

**Table 2**

Analytical performance data of the proposed method after microextraction of metal ions with silica-modified magnetite NPs.

Metal ion	Dynamic linear range (ng L <sup>-1</sup> )	Detection limits (ng L <sup>-1</sup> )	Correlation coefficient (R)	RSD% (n = 6) <sup>a</sup>
Cu	14–190	4.7	0.9980	2.4 (60)
Co	26–250	9.1	0.9946	3.1 (100)
Ni	27–250	9.5	0.9949	3.6 (100)
Cd	7–110	2.3	0.9978	2.8 (50)
Pb	22–220	7.4	0.9972	2.8 (95)
Mn	45–400	15.3	0.9953	2.3 (170)

<sup>a</sup> Numbers in parentheses represent the concentrations, at which RSDs were calculated.

desorption ability of methanol, as experimentally proved, was slightly inferior to a methanolic solution of 1 N HNO<sub>3</sub>. Also, our results showed that an aliquot of 250 µL of methanolic solution of 1 N HNO<sub>3</sub> can conveniently desorb the complexed metals and prepare the sample for injection into the graphite furnace of AAS, maintaining high preconcentration capacity.

### 3.2.7. Effect of ionic strength

The ionic strength of the working solution was varied from 0 to 0.2 M NaNO<sub>3</sub>. The extracted amount of metal ions diminished with the increase in ionic strength, as illustrated in Fig. 5. The role of electrostatic attraction in the adsorption process was significant and the competition between sodium and CPBr cations for the negative surface of NPs caused the formation of mixed surfactant aggregates on the magnetite NPs surface to abate. Besides, as the ionic strength increases, the cmc decreases and the size of the micelles increases for cationic surfactants causing the micelles to be formed at lower concentrations of CPBr.

### 3.3. Analytical figures of merit

To explore their capability, silanized magnetite NPs were used to extract trace amounts of metals from surface water prior to ETAAS determination. Quality parameters of the proposed method under optimum conditions are tabulated in Table 2. The microextraction method allows quantification of metal ions with good linearity ( $R=0.9946–0.9980$ ) in the range of 14–400 ng L<sup>-1</sup>. Detection limits, calculated as three times the standard deviation of ten replicate measurements of the blank, were found to be 4.7–15.3 ng L<sup>-1</sup>. The relative standard deviation, calculated from six replicate experiments on the same day, was less than 3.6%.

The accuracy of the proposed method was tested by calculating the recovery of the heavy metal ions from spiked tap and river water samples. The obtained recoveries for the heavy metal ions, as the mean values ( $n=3$ ), are in the acceptable range of 93–113% (Table S1 of Supplementary Material).

## 4. Conclusions

Encouraged by the outstanding properties of magnetite NPs and their silica-modified counterparts already mentioned, we report here the concept of the preconcentration of metals from tap water and surface water in connection with a cationic surfactant and a complexing agent. The strong hydrophobic interactions between the mixed hemimicelles and complexed metals made this new microextraction method possess high extraction efficiency and capacity. The preconcentration method described herein using 8-HQ, CPBr and silica-modified magnetite NPs for the determination of Cu, Co, Ni, Cd, Pb, Mn in water samples exhibited fairly good analytical performance as expressed by the acceptable accuracy, repeatability and sensitivity. Silica-coated magnetic NPs constitute a low-cost absorbing phase and in combination with surfactant-

based adsorption capacity it can be used for the preconcentration of metals. In addition, the proposed method provided a rapid, efficient sample preparation process and was able to treat large-volume samples in a short period avoiding the time-consuming column passing and filtration steps. Conceivably, the developed method can be applied using any ICP-based instrumentation to determine simultaneously a wide gamut of metals.

## Acknowledgements

The authors are grateful to Assist. Prof. D. Petrakis and Assoc. Prof. J. Plakatouras for their assistance to obtain the surface area data and FT-IR spectra, respectively.

## Appendix A. Supplementary data

Supplementary data associated with this article can be found, in the online version, at doi:10.1016/j.talanta.2011.02.013.

## References

- [1] A.-H. Lu, E.L. Salabas, F. Schüth, *Angew. Chem. Int. Ed.* 46 (2007) 1222–1244.
- [2] K.M. Krishnan, A. Pakhomov, Y. Bao, P. Blomquist, Y. Chun, M. Gonzales, K. Griffin, X. Ji, B. Roberts, *J. Mater. Sci.* 41 (2006) 793–815.
- [3] J. Hu, G. Chen, I.M.C. Lo, *Water Res.* 39 (2005) 4528–4536.
- [4] T. Tuutijärvi, J. Lu, M. Sillanpää, G. Chen, *J. Hazard. Mater.* 166 (2009) 1415–1420.
- [5] C.T. Yavuz, J.T. Mayo, W.W. Yu, A. Prakash, J.C. Falkner, S. Yean, L. Cong, H.J. Shipley, A. Kan, M. Tomson, D. Natelson, V.L. Colvin, *Science* 314 (2006) 964–967.
- [6] B. Hai, J. Wu, X. Chen, J.D. Protasiewicz, D.A. Scherson, *Langmuir* 21 (2005) 3104–3105.
- [7] W. Yantasee, C.L. Warner, T. Sangvanich, R.S. Addleman, T.G. Carter, R.J. Wiacek, G.E. Fryxell, C. Timchalk, M.G. Warner, *Environ. Sci. Technol.* 41 (2007) 5114–5119.
- [8] P.-C. Lin, M.-C. Tseng, A.-K. Su, Y.-J. Chen, C.-C. Lin, *Anal. Chem.* 79 (2007) 3401–3408.
- [9] M. Yamaura, R.L. Camilo, L.C. Sampaio, M.A. Macedo, M. Nakamura, H.E. Toma, *J. Magn. Magn. Mater.* 279 (2004) 210–217.
- [10] S. Čampelj, D. Makovec, M. Drogenik, J. Magn. Magn. Mater. 321 (2009) 1346–1350.
- [11] D.M. Souza, A.L. Andrade, J.D. Fabris, P. Valurio, A.M. Góes, M.F. Leite, R.Z. Domingues, *J. Non-Cryst. Solids* 354 (2008) 4894–4897.
- [12] Y. Liu, L. Jia, *Microchem. J.* 89 (2008) 72–76.
- [13] C. Huang, B. Hu, *Spectrochim. Acta Part B* 63 (2008) 437–444.
- [14] L. Zhang, Y. Zhai, X. Chang, Q. He, X. Huang, Z. Hu, *Microchim. Acta* 165 (2009) 319–327.
- [15] S.C. Pang, S.F. Chin, M.A. Anderson, *J. Colloid Interface Sci.* 311 (2007) 94–101.
- [16] A.-H. Lu, E.L. Salabas, F. Schüth, *Angew. Chem. Int. Ed.* 46 (2007) 1222–1244.
- [17] X.L. Zhao, J.D. Li, Y.L. Shi, Y.Q. Cai, S.F. Mou, G.B. Jiang, *J. Chromatogr. A* 1154 (2007) 52–59.
- [18] T.M. Holsen, E.R. Taylor, Y.C. Seo, P.R. Anderson, *Environ. Sci. Technol.* 25 (1991) 1585–1589.
- [19] L. Lunar, S. Rubio, D. Pérez-Bendito, *Analyst* 131 (2006) 835–841.
- [20] G.-L. Chen, S.-Y. Suen, S. Vied, K. Pickering, C. Perrin, E.D. Conte, *Analyst* 134 (2009) 331–336.
- [21] S. Laurent, D. Forge, M. Port, A. Roch, C. Robic, L. Vander Elst, R.N. Muller, *Chem. Rev.* 108 (2008) 2064–2110.
- [22] Y. Song, S. Zhao, P. Tchounwou, Y.-M. Liu, *J. Chromatogr. A* 1166 (2007) 79–84.
- [23] X. Zhao, Y. Shi, Y. Cai, S. Mou, *Environ. Sci. Technol.* 42 (2008) 1201–1206.
- [24] X. Zhao, Y. Shi, T. Wang, Y. Cai, G. Jiang, *J. Chromatogr. A* 1188 (2008) 140–147.
- [25] J. Li, X. Zhao, Y. Shi, Y. Cai, S. Mou, G. Jiang, *J. Chromatogr. A* 1180 (2008) 24–31.
- [26] L. Zhu, D. Pan, L. Ding, F. Tang, Q. Zhang, Q. Liu, S. Yao, *Talanta* 80 (2010) 1873–1880.
- [27] C.D. Stalikas, *Trends Anal. Chem.* 21 (2002) 343–355.
- [28] E. Paleologos, C.D. Stalikas, G.A. Piliidis, S.M. Tzouwara-Karayanni, M.I. Karayannis, *J. Anal. At. Spectrom.* 15 (2000) 287–291.
- [29] J. Stary, *Anal. Chim. Acta* 28 (1963) 132–149.
- [30] S. Giri, B.G. Trewyn, M.P. Stellmaker, V.S.-Y. Lin, *Angew. Chem. Int. Ed.* 44 (2005) 5038–5044.
- [31] J. Shen, A.D. Ebner, J.A. Ritter, *J. Colloid Interface Sci.* 214 (1999) 333–343.
- [32] X. Huang, J. Yang, W. Zhang, Z. Zhang, Z. An, *J. Chem. Educ.* 76 (1999) 93–94.
- [33] M. Yamaura, R.L. Camilo, L.C. Sampaio, M.A. Macêdo, M. Nakamura, H.E. Toma, *J. Magn. Magn. Mater.* 279 (2004) 210–217.
- [34] L.S. Clesceri, A.E. Greenberg, A.D. Eaton (Eds.), *Standard Methods for the Examination of Water and Wastewater*, 20th ed., APHA, Washington, DC, 1998.
- [35] J.A. Schwarz, C.T. Driscoll, A.K. Bhanot, *J. Colloid Interface Sci.* 97 (1984) 55–61.
- [36] T.P. Goloub, L.K. Koopal, B.H. Bijsterbosch, M.P. Sidorova, *Langmuir* 12 (1996) 3188–3194.
- [37] A. Goswami, A.K. Singh, B. Venkataramani, *Talanta* 60 (2003) 1141–1154.